Improved Optimal Power Flow for a Power System Incorporating Wind Power Generation by Using Grey Wolf Optimizer Algorithm

Sebaa HADDI, Omrane BOUKETIR, Tarek BOUKTIR

Department of Electrical Engineering, Faculty of Technology, University of Setif, El Bez, 19000 Setif, Algeria

sebaa_73@yahoo.fr, Omrane@univ-setif.edu.dz, tarek.bouktir@esrgroups.org

DOI: 10.15598/aeee.v16i4.2883

Abstract. *In this paper, an efficient Grey Wolf Optimizer (GWO) search algorithm is presented for solving the optimal power flow problem in a power system, enhanced by wind power plant. The GWO algorithm is based on meta-heuristic method, and it has been proven to give very competitive results in different optimization problems. First, by using the proposed technique, the system independent variables such as the generators' power outputs as well as the associated dependent variables like the bus voltage magnitudes, transformer tap setting and shunt VAR compensators values are optimized to meet the power system operation requirements. The Optimal power flow study is then performed to assess the impact of variable wind power generation on system parameters. Two standard power systems IEEE30 and IEEE57 are used to test and verify the effectiveness of the proposed GWO method. The obtained results are then compared with others given by available optimization methods in the literature. The outcome of the comparison proved the superiority of the GWO algorithm over other meta-heuristics techniques such as Modified Differential Evolution (MDE), Enhanced Genetic Algorithm (EGA), Particle Swarm Optimization (PSO), Biogeography Based Optimization (BBO), Artificial Bee Algorithm (ABC) and Tree-Seed Algorithm (TSA).*

Keywords

Grey Wolf Optimizer (GWO), grey wolves, OPF problem.

1. Introduction

Optimal power flow problem has been studied for many years and has become one of the most important means used for adjusting optimal settings of power systems. Therefore, it has received more attention from many researchers throughout the world [1]. Several optimization techniques have been used to solve this problem, in order to find the optimal solution for operational objective functions in a power system, such as fuel cost, voltage profile and voltage stability enhancement. Some methods are based on nonlinear programming, quadratic programming, Newton techniques and interior point. These methods have many drawbacks, such as high complexity, convergence to local optimum and sensitivity to initial conditions [2].

Intelligent search methods such as meta-heuristic optimization techniques have been introduced to overcome some optimization problems encountered with classical methods. The most popular ones are; Genetic Algorithm (GA), Particle Swarm Optimization (PSO), Simulated Annealing (SA), Evolutionary Programming (EP), Artificial Bee Colony algorithm (ABC), Ant Colony Optimization (ACO), Differential Evolution (DE). Based on these original methods new derived techniques have been obtained and used in OPF problem as in ABC [3], EGA [4], gradient method and General Algebraic Modeling System (GAMS) [5], Efficient Evolutionary Algorithm (EEA) [5], Evolving Ant Direction Differential Evolution (EADDE) [6], Differential Search Algorithm (DSA) [7], CSA [8], Krill Herd Algorithm (KHA) [9], Simulated Annealing (SA) [10], Interior Search Algorithm (ISA) [11], Enhanced Genetic Algorithm (EGA) [12], BBO [13], PSO [14], Gravitational Search Algorithm (GSA) [15], Genetic evolving ant direction PSODV hybrid algorithm (PSODV) [16], Real Coded Biogeography-Based Optimization RC-BBO [17] and Evolutionary Algorithm (EA) [18]. Most of these methods are recently extensively used in solving global optimization searching problems and have been giving promising results beside that they have attractive characteristics, such as easy implementation and fast convergence [18].

A common drawback to meta-heuristic methods is that, in general, the optimization performance is highly dependent on fine parameter tuning. However, the proposed approach outperforms these methods in term of convergence speed to the best solution. Moreover, the use of OPF is extended to include the study of renewable energy systems like wind power, which becomes more and more useful in recent power networks, and many studies are made to integrate this natural power efficiently to a power system. Ranjit and Jadhav in [19], as well as Maskar et al. in [20], presented a study of OPF problem in a system incorporating wind power sources, using modified ABC algorithm named Gbest guided ABC algorithm; the method showed good results for fuel cost optimization case, and voltage profile enhancement, then under wind condition the total operating cost is optimized efficiently, compared to other methods. The method presented some benefits concerning reserve coefficient adjustment when considering imbalance cost of wind power. Meanwhile, Shanhe et al. [21] presented a new economic dispatch technique based on PSO-GSA algorithm for a power system including two wind power sources; the method was tested on a six generators' system connected with two stochastic wind power sources. The test yielded good results compared with other results found in the literature with different methods especially for cost and emission reduction. Panda and Tripathy [22], and Mishra and Vignesh [23] introduced another OPF algorithm based on security constrained OPF solution of wind-thermal generation system using modified bacteria foraging algorithm. The method was tested on the same system stated in [18], in which the wind power variability was modelled incorporating conventional thermal generating system. Recent works in [19], [24] and [25] presented better results and faster convergence characteristics using Grey Wolf Optimizer algorithm. Grey Wolf Optimizer (GWO) algorithm mimics the behaviour of grey wolves in nature by simulating their leadership hierarchy, through haunting, searching for, encircling, and attacking the prey [26].

The present paper aims to investigate the efficiency of GWO algorithm, as a new meta-heuristic population-based algorithm. It presents a solution to the OPF problem of a power system incorporating wind power generation. The rest of the paper is organized as follows; after the introduction, the OPF problem formulation is given in Sec 2. Subsec. 2.2. deals with the OPF problem incorporating wind power. Section 3. presents the GWO algorithm and associated simulation steps for solving the OPF problem. In Sec. 4. simulation results using GWO algorithm are presented and analysed. Section 5. concludes the study.

2. OPF Problem Formulation

2.1. Optimal Power Flow

The objective of conventional OPF problem is to minimize fuel cost for power generation by determining a set of control variables while satisfying system equality and inequality constraints. The OPF problem is formulated by [27]:

$$\min f(x,u), \tag{1}$$

$$s \cdot tg(x,u) = 0, \tag{2}$$

$$h(x,u) \leq 0, \tag{3}$$

where $[\vec{x}]$: is the vector of dependent variables consisting of slack bus PG_1, load bus voltage V_L, generator reactive power outputs Q_G, and transmission line loading S_L. This vector is expressed by:

$$X^T = [P_{G1}, V_{L1}, ..V_{ND}, Q_{G1}, ..Q_{GN}, S_{l1}, ..S_{l_{NL}}], \tag{4}$$

where ND, NG and NL are number of load buses, number of generators, and number of transmission lines, respectively.

$[\vec{u}]$ is the vector of independent variables consisting of generator voltages V_G, generator real power outputs P_G except at the slack bus P_{G1}, transformer tap settings T_P, shunt VAR compensation Q_C. This vector is expressed by:

$$\vec{u}^T = [V_{G1}, ..V_{NG}, .P_{G2}..P_{GN}, T_{P1}, ..T_{P_{NT}}, Q_{C1}, ..Q_{C_{NC}}], \tag{5}$$

where: NG, NT, and NC are the number of thermal generators, regulating transformers, shunt compensators, respectively.

1) Fuel Cost Optimization

The function f from Eq. (1) concerned in the OPF study represents the total generation cost formulation and it is as:

$$f(P_{gi}) = \sum_{i=1}^{NG} a_i P_{gi}^2 + b_i P_{gi} + c_i \quad (\$/h). \tag{6}$$

When considering valve effect, the function f; is rewritten as:

$$\begin{gathered} f(P_{gi}) = \sum_{i=1}^{NG} a_i P_{gi}^2 + b_i P_{gi} + \\ + c_i \mid d_i(\sin(e_i(P_{gi\min} - P_{gi} \quad (\$/h), \end{gathered} \tag{7}$$

where: a_i, b_i, c_i, d_i and e_i are fuel cost coefficients of i^{th} thermal generating unit.

2) Voltage Profile Improvement

The aim of this objective function is to minimize the load bus voltage deviations from the reference value which is 1 per unit; this function is expressed by:

$$VD = \sum_{i=1}^{N_{PQ}} | V_i - V_{ref} |, \tag{8}$$

where: VD represents the voltage deviation in (p.u); V_i is the i^{th} load bus voltage; and V_{ref} is the reference voltage which is taken here to be 1 p.u, and thus the objective function Eq. (6) becomes as follows:

$$\begin{aligned} f(P_{gi}) = &\sum_{i=1}^{NG} (a_i P_{gi}^2 + b_i P_{gi} + c_i) + \\ &+ w \sum_{i=1}^{N_{PQ}} | V_i - 1 |, \end{aligned} \tag{9}$$

where: w represents a weighting factor selected by the user; many works are choosing w to be 100 in order to keep the variable within the designed limits, as in [1] and [15].The OPF equality constraint such as the active power balance equation is expressed by:

$$\sum_{i=1}^{NG} P_{Gi} = P_d + P_l, \tag{10}$$

where: P_d represents the load of the system, and P_l is the total active power loss.

3) OPF Incorporating Inequality Constraints

In order to handle the inequality constraints of dependent variables, including slack bus real and reactive power, load bus voltage magnitudes and transmissions line loading; the problem is transformed into unconstrained OPF problem by penalizing these quantities using the penalty function defined as:

$$h(x_i) = \begin{cases} (x_i - x_{i\,\max}) & \text{if } x > x_{i\,\max}, \\ (x_{i\,\min} - x_i)^2 & \text{if } x < x_{i\,\max}, \\ 0 & \text{if } x_{i\,\min} \le x_i \le x_{i\,\max}. \end{cases} \tag{11}$$

where: $h(x_i)$ is the penalty function of variable x_i, here the x_i represents dependent variables, $x_{i\,\min}$ and $x_{i\,\max}$ are the upper and lower limits of x_i variable, respectively.

The value of the penalty function grows with a quadratic form when the constraints are violated, and equals to zero if the constraints are not violated, while the extended objective function Eq. (6) can be rewritten as:

$$\begin{aligned} f(P_{gi}) = &\sum_{i=1}^{NG} f_i + \eta_P (P_{g1} - P_{g1}^{\lim})^2 + \eta_Q (Q_{g1} - Q_{g1}^{\lim})^2 \\ &+ \eta_V \textstyle\sum_{i=1}^{NL} (V_{Li} - P_{Li}^{\lim})^2 + \eta_S \displaystyle\sum_{i=1}^{NB} (S_{it} - P_{it}^{\lim})^2, \end{aligned} \tag{12}$$

where: η_p, η_q, η_v and η_s are penalty factors or weights of active power generation of slack bus, reactive power output of generator buses, PQ bus magnitudes and transmission line loadings respectively. Their values are generally taken to be 100 for the same reason in Eq. (9) [14], [15], [16] and [17].

2.2. OPF Problem Formulation with Wind Power

The fuel cost objective in Eq. (6) is augmented with the cost associated with stochastic wind power, as in Eq. (13) [28]

$$\begin{aligned} F_T = &\sum_{i=1}^{NG} a_i P_{gi}^2 + b_i P_{gi} + c_i + \\ &+ F(P_{wj}) + C_{wj} \quad (\$/h), \end{aligned} \tag{13}$$

where; $F(P_{wj})$ is the cost for generation of wind power which is directly proportional to the wind power output and is given by:

$$F(P_{wj}) = d_j \times P_{wj} \quad (\$/h), \tag{14}$$

d_j: is the direct cost coefficient of non-utility service, which equals to zero for the utility services.

C_{wj}: represents the imbalance cost of investment in j^{th} wind power source due to two components as in Eq. (15) [29]:

$$\begin{aligned} C_w = &\sum_{j=1}^{N_w} (K_{p,j} \times W_{j,ue}) + \\ &+ \sum_{j=1}^{N_w} (K_{R,j} \times W_{j,oe}) \quad (\$/h), \end{aligned} \tag{15}$$

where: $W_{j,ue}$ and $W_{j,oe}$, are given by the following expressions:

$$W_{j,ue} = \left(\begin{aligned} &(P_{wr,j} - P_{wj}) \left[\exp\left(- \left(\frac{v_{r,j}^{kj}}{c_i^{kj}} \right) \right) \right. \\ &\left. - \exp\left(- \left(\frac{v_{o,j}^{kj}}{c_i^{kj}} \right) \right) \right] + \left(\frac{P_{wr,j} v_{in,j}}{v_{r,j} - v_{in,j}} \right. \\ &\left. + P_{wj} \right) \left[\exp\left(- \left(\frac{v_{r,j}^{kj}}{c_i^{kj}} \right) \right) \right. \\ &\left. - \exp\left(- \left(\frac{v_{1,j}^{kj}}{c_i^{kj}} \right) \right) \right] + \frac{P_{wr,j} v_{in,j}}{v_{r,j} - v_{in,j}} \\ &\cdot \left\{ \Gamma \left[1 + \frac{1}{k_i}, \left(\frac{v_{1,j}^{kj}}{c_i^{kj}} \right)^{kj} \right] \right. \\ &\left. - \Gamma \left[1 + \frac{1}{k_i}, \left(\frac{v_{r,j}^{kj}}{c_i^{kj}} \right)^{kj} \right] \right\} \end{aligned} \right), \tag{16}$$

$$W_{j,oe} = \left(\begin{array}{c} (P_{wr,j}) \left[1 - \exp\left(- \left(\frac{v_{in,j}^{kj}}{c_i^{kj}} \right) \right) \right. \\ \left. - \exp\left(- \left(\frac{v_{o,j}^{kj}}{c_i^{kj}} \right) \right) \right] + \left(\frac{P_{wr,j} v_{in,j}}{v_{r,j} - v_{in,j}} \right. \\ \left. + P_{wj} \right) \left[\exp\left(- \left(\frac{v_{r,j}^{kj}}{c_i^{kj}} \right) \right) \right. \\ \left. - \exp\left(- \left(\frac{v_{1,j}^{kj}}{c_i^{kj}} \right) \right) \right] + \frac{P_{wr,j} v_{in,j}}{v_{r,j} - v_{in,j}} \\ \cdot \left\{ \Gamma \left[1 + \frac{1}{k_i}, \left(\frac{v_{1,j}^{kj}}{c_i^{kj}} \right)^{kj} \right] \right. \\ \left. - \Gamma \left[1 + \frac{1}{k_i}, \left(\frac{v_{r,j}^{kj}}{c_i^{kj}} \right)^{kj} \right] \right\} \end{array} \right), \quad (17)$$

where: $v_1 = v_{in,j} + (v_{r,j} - v_{in,j}) P_{W,j} / P_{Wr,j}$; $k > 0$, $c > 0$ are the shape factor and scale factor, respectively. P_{Wr}; is the available active power for the j^{th} wind turbine. $P_{Wr,j}$, is the rated wind power output, $P_{W,j}$ is the actual wind power output of j^{th} wind turbine. V_{in}, V_0 and V_r are the cut-in, cut-off and rated wind speed, respectively.

Equation (15) represents the stochastic nature of wind power output for which the following parameters are associated:

- $K_{p,j}$: penalty cost coefficient for not using all available power from j^{th} wind turbine due to under-generation estimated from j^{th} wind turbine,
- $K_{R,j}$: reserve cost coefficient due to the reserve capacity used to compensate the over-estimated wind power of j^{th} wind turbine.
- $W_{j,ue}$ and $W_{j,oe}$, are the expected value of j^{th} wind turbine for over-estimated and under-estimated energy output which was calculated using Eq. (16) and Eq. (17) [2].

To deal with wind speed variations of wind turbine, the generated power from wind can be approximated with respect to particular wind speed V, as follows [2]:

$$P_w(V) = \begin{cases} 0 & V \leq V_{in}, \\ aV^3 + bV^2 + cV + d & V_r > V > V_{in}, \\ P_{we} & V_{off} > V \geq V_r, \\ 0 & V \geq V_{off}. \end{cases} \quad (18)$$

$P_w(V)$ is the available wind power output, a, b, c, and d; are constants, in this study the generated wind power output is used as negative real power load connected at special bus in the test system.

1) System Equality Constraints with Wind Energy

The equality constraints for the case of wind power are expressed by [26]:

$$\sum_{i=1}^{NG} P_{Gi} + \sum_{j=1}^{N_w} P_{Wj} = P_d + P - l. \quad (19)$$

The active power losses are given by the formula:

$$P_{loss} = \sum_{n=1}^{Nl} G_{nij} \left[| V_i |^2 + | V_j |^2 - 2 | V_i || V_j | \cos(\delta_i - \delta_j) \right], \quad (20)$$

where: i and j are the sending and receiving ends of particular line n. Nl; is the number of lines. The equality constraints from Eq. (8) and Eq. (9) are rewritten for the wind node j as:

$$P_{Wj} - P_{dj} - P_{j,cal}(V, \delta) = 0, \quad (21)$$

$$Q_{Wj} - Q_{dj} - Q_{j,cal}(V, \delta) = 0. \quad (22)$$

The control variables vector is modified as:

$$\vec{u}^T = [V_{G1}, ..V_{NG}, .P_{G2}..P_{GN}, P_{w1}, ..P_{N_w}, T_{p1}, ..T_{pNT}, Q_{C1}, ..Q_{C_{NC}}], \quad (23)$$

where: N_W represents the number of wind generators in the power system network.

2) Wind Generators Constraints

In addition to the precedent inequality constraints, we can write;

$$0 \leq P_{Wi} \leq P_{Wr,i}, \quad i = 1, ..N_w, \quad (24)$$

where: P_{Wr}, is the rated active power output of the i^{th} wind turbine unit.

3) Spinning Reserve Constraints Model for OPF with Wind Energy

The spinning reserve is the reserve capacity used for sudden load increase, unpredictable fall in wind power output or forced outage of thermal generators units. The spinning reserve has two limits which are the upper and lower limits that represent system up and system down spinning reserves USR and DSR; given by the following expressions: [2] and [30]:

$$P_{US} \geq R_{USR} + r\% \times \sum_{j=1}^{N_w} P_{W,j}, \quad (25)$$

$$P_{DS} \geq R_{DSR} \times s\% + r\% \times \sum_{j=1}^{N_w} P_{W,j}, \quad (26)$$

where; r is the influence coefficient that gives the percentage of wind power contributing to USR and DSR. The USR can be represented with respect to the total load and total wind power by:

$$\sum_{i=1}^{N} P_{US_i} \geq P_d \times s\% + r\% \times P_{WT}, \qquad (27)$$

where: US_i represents the maximum up spinning reserve limit of i^{th} thermal unit, and s is the percentage of load contributing to USR, these constraints will be considered during the implementation of GWO algorithm. As the rate of wind power penetration increases, it becomes more difficult to predict the exact amount of power injected by all generators into the power grid. This added more uncertainty when accounting the spinning reserve requirements.

3. Used Algorithm

3.1. GWO Algorithm

Grey Wolf Optimizer (GWO) is a new algorithm proposed by Mirjalili et al. in 2014 [31]. This algorithm mimics the leadership hierarchy and hunting technique used by grey wolves to catch their prey until stopping its movement. GWO is similar to other population-based meta-heuristic algorithms, by simulating the natural behavior of grey wolves in their social life when searching for food; they follow hierarchy structure in the group (Fig. 1). The first level representing the leaders of the group is called (alpha), the second level in the hierarchy of grey wolves is (beta) which helps alpha to make decisions. The next levels are delta and omega; they are the lowest ranks in the group; they have to eat after all levels. In fact, these wolves are group-hunting that take three main steps; chasing, encircling and attacking. The algorithm starts with a given number of wolves whose positions are randomly generated.

3.2. Steps of GWO Algorithm

Four types of wolves groups can be used to simulate the leadership hierarchy of grey wolves. This hierarchy is represented in Fig. 1, respecting the social dominant degree, the high class is named alpha (α), mostly responsible for making decisions about hunting and order the other wolves in the pack.

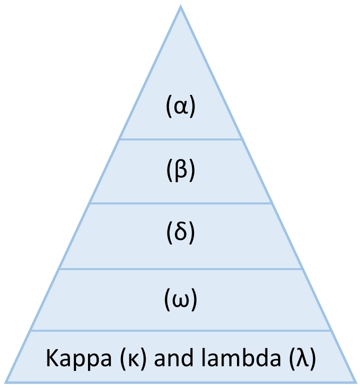

Fig. 1: Hierarchy levels of grey wolves.

Fig. 2: (a) attacking prey (b) hunting prey by wolves.

They can be considered as the fittest solution. The next level in the chain is called beta (β), the wolves of this level help the alpha ones in supervising other groups' actions. They can replace the alpha wolves when they die or become aged and begin to be the best candidate solution. The lowest ranking grey wolves are delta (δ) wolves and omega (ω) wolves [27] and [32]. Therefore types α, β, and δ leading the optimization (hunting) process, while ω group is to track them. Kappa (κ) and lambda (λ) wolves are directed by omega in the hierarchy.

The main steps involved in the original GWO algorithm are as follows:

- Initialize the search agents.
- Assign Alpha, Beta and Gamma by fitness.
- Encircling the prey: represent the circular area around the best solution (prey). This step can be represented by the following equations:

$$D = \mid C \cdot \vec{X}_p(t) - X(t) \mid, \tag{28}$$

$$X(t+1) = \mid \vec{X}_p(t) - A \cdot D \mid, \tag{29}$$

where: $\vec{X}_p$ is the prey's position vector. $(\vec{A})$ and $(\vec{C})$, are vectors given by the following equations:

$$a = 2(1 - t/T_{\max}), \tag{30}$$

$$\vec{A} = 2 \cdot ar_1 - a, \tag{31}$$

$$\vec{C} = 2r_2, \tag{32}$$

where: t is the current iteration and $T_{\max}$, total iterations.

The parameter a decreases linearly in the range of $[2, 0]$ for successive iterations using Eq. (30); that model wolfs behaviour approaching the prey; r_1 and r_2 are random vectors in the range $[0, 1]$.

- Hunting step: the encircling process comes to the second step involving hunting guided by the alpha wolf group. The following equations represent this step:

$$D_\alpha = \mid C_1 \cdot X_\alpha(t) - X(t) \mid, \tag{33}$$

$$D_\beta = \mid C_2 \cdot X_\beta(t) - X(t) \mid, \tag{34}$$

$$D_\delta = \mid C_3 \cdot X_\delta(t) - X(t) \mid, \tag{35}$$

$$X_1 = X_\alpha - A_1 \cdot D_\alpha X_2, \tag{36}$$

$$X_2 = X_\beta - A_2 \cdot D_\beta X_3, \tag{37}$$

$$X_3 = X_\delta - A_3 \cdot D_\delta, \tag{38}$$

$$X(t+1) = (x_1 + X_2 + X_3)/3. \tag{39}$$

- Attacking the prey: Firstly, r_1 and r_2 are randomly selected for mutation (A and C), then the base vector (X) is randomly selected within the range $[r_1, r_2]$, that is to drive the algorithm to global solution and avoid local optima. The fact that "a" decreases from 2 to 0 makes the exploration more efficient, but slows down the GWO convergence characteristics. So, the final step of attacking the prey is done by decreasing linearly the value of "a" from 2 to 0 [33].
- Steps 2 to 5 are then repeated until the maximum number of iterations is reached.

3.3. Pseudo Code for GWO Algorithm

Initialize *the grey wolf population;* Xi*; i=1. . . n*
Initialize *parameters; a, A, and C*
Calculate *the fitness of each Search_ Agent;*
X_a *=the best search agent;*
X_β *=the second best search agent;*
X_δ *the third best search agent;*
While *Iter≤ Max_ Iter*
For *j∈{search space}*
Sort *the population of grey wolves according to their fitness*
Update *the Update the position of the current Search Ahent using Eq. (39);*
endfor *% search space*
Update *a, A and C*
Calculate *the fitness of the new search agents;*
Update X_a , X_β *and* X_δ
Iter=Iter+1;
End*; Return, Best solution found so far* X_a*;*

4. Case Study and Simulation Results

In this section, the optimal power flow problem is implemented using GWO algorithm and two case studies are considered. For the first case study, the simulation is carried out on IEEE30- bus system as used in [34], by solving conventional OPF and considering quadratic model of thermal generators cost using Eq. (6). Then, the OPF problem is implemented considering wind power for a given wind speed and cost profiles. Later, the OPF problem is implemented considering different wind speed profiles.

In the second case study, the simulation is carried out on IEEE57-bus system. The purpose of these studies is to validate the results obtained using GWO algorithm by comparing them with the results available in the literature.

4.1. Case Study N°1: IEEE30 Bus Test System

1) Case 1.1: OPF with Quadratic Fuel Cost

The objective function for this case study is given by Eq. (6), for all thermal generators units, the numerical data and parameters are taken from [35], the PQ bus voltages are between 0.95 and 1.05 p.u, the shunt Var Compensator are not considered in this case study, except for the two shunt capacitors banks, at nodes 10 and 24 of 19 and 4.3 Mvars respectively. The optimum control settings obtained by using GWO algorithm are presented in Tab. 1.

Tab. 1: Optimal power flow without considering dependent variables.

Control variables	Lower/up per limits	Case 1.1	Case 1.2	Case 1.3
P1(MW)	50 200	176.1721	176.472	199.988
P2	20 80	48.0926	48.795	20.0000
P5	15 35	21.1376	21.506	15.0152
P8	10 30	23.3591	21.799	10.0000
P11	10 30	11.3591	11.993	10.0000
P13	12 40	12.0000	12.000	12.0000
V1	0.95 - 1.05	1.0600	1.0600	1.06000
V2	0.95 - 1.10	1.0512	1.0512	1.0512
V5	0.95 - 1.10	1.0224	1.0224	1.0224
V8	0.95 - 1.10	1.0333	1.0333	1.0333
V11	0.95 - 1.10	1.0820	1.0820	1.0820
V13	0.95 - 1.10	1.0910	1.0910	1.0910
T11	0.90 - 1.10	1.0150	1.0150	1.0170
T12	0.90 - 1.10	0.9070	0.9070	0.9070
T13	0.90 - 1.10	0.9680	0.9680	0.9680
T14	0.90 - 1.10	0.9550	0.9550	0.9550
Fuel cost \$/h	-	**801 .1769**	**804 .4726**	**910 .6575**
Power loss	-	**9.1528**	**9.202**	**12.709**
Voltage deviations	-	**0.10**	**0.1082**	-

In order to assess the potential of the proposed approach, a comparison between the obtained results of fuel cost and those reported in the literature has been carried out. The results of this comparison are given in Tab. 2. It is worth mentioning that the comparison has been carried out with the same test system data.

Different OPF results of active generation powers and losses for different case studies are given in Tab. 1.

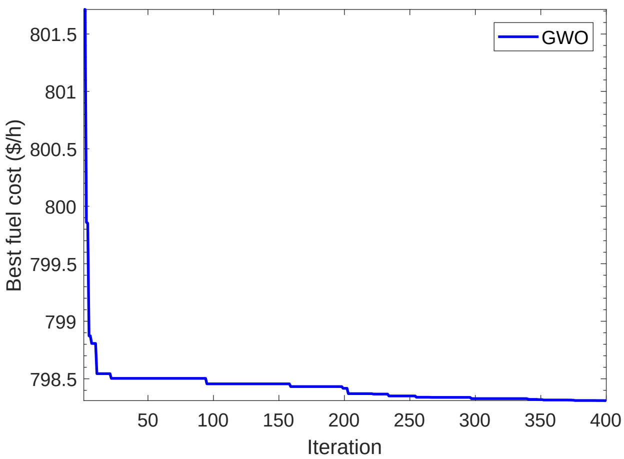

Fig. 3: Convergence characteristic of IEEE30 bus system case 1.1.

The best fuel cost calculated by the proposed algorithm for this case is 801.1769 \$/h, which is better than

Tab. 2: Comparison of quadratic fuel cost case 1.1.

Methods	Fuel cost (\$/h)
MDE [35]	802.376
ABC [3]	802.305
EGA [4]	802.060
GAMS [5]	801.519
GWO	**801.176**

that obtained by many other algorithms as depicted in Tab. 2. The corresponding convergence graph is shown in Fig. 3.

Tab. 3: Optimal power flow considering dependent variables.

Control variables	Lower/up per limits	Case 1.1	Case 1.2	Case 1.3
P1 (MW)	50 200	176.9340	176.953	199.636
P2	20 80	48.7328	48.8151	20.0000
P5	15 35	21.2692	21.2488	22.2126
P8	10 30	21.0177	21.0724	25.1402
P11	10 30	11.8525	11.7632	13.2466
P13	12 40	12.0000	12.0000	12.2392
V1(p.u)	0.95 - 1.05	1.0999	1.0999	1.0999
V2	0.95 - 1.10	1.0885	1.0885	1.0885
V5	0.95 - 1.10	1.0631	1.0631	1.0631
V8	0.95 - 1.10	1.0712	1.0712	1.0712
V11	0.95 - 1.10	1.0998	1.0998	1.0998
V13	0.95 - 1.10	1.0733	1.0733	1.0733
C10 (Mvars)	0.00 - 5.00	4.1669	4.1669	4.1669
C15	0.00 - 5.00	0.2398	0.2398	0.2398
C17	0.00 - 5.00	4.2017	4.2017	4.2017
C20	0.00 - 5.00	0.1489	0.1489	0.1489
C21	0.00 - 5.00	0.6478	0.6478	0.6478
C22	0.00 - 5.00	4.2499	4.2499	4.2499
C23	0.00 - 5.00	1.3886	1.3886	1.3886
C24	0.00 - 5.00	2.1815	2.1815	2.1815
C29	0.00 - 5.00	2.0780	2.0780	2.0780
T11	0.90 - 1.10	1.0461	1.0150	1.0170
T12	0.90 - 1.10	0.9000	0.9070	0.9070
T13	0.90 - 1.10	0.9997	0.9680	0.9680
T14	0.90 - 1.10	0.9642	0.9550	0.9550
Fuel cost (\$/h)	-	**798.3107**	**806.1530**	**916.6968**
Power loss (MW)	-	**8.4061**	**8.4526**	**9.0762**
Voltage deviations	-	0.422	**0.077**	0.078

For the methods EADDE in [6], GABC in [7], EEA in [5], CSA in [8], KHA in [9], SA in [10], and ISA in [11], the PQ bus voltages are between 0.95 and 1.1 p.u, the transformers tap setting and shunt Var compensators are considered in the same case study, and the generator voltages are taken close to their high permissible limit. Table 3 shows the corresponding optimal power flow results when using the optimal settings of dependent variables. It can be observed from Tab. 4 that GWO algorithm gives better results. The system reactive generation powers for this case study are within their specified limits as in Tab. 5. Table 6 presents a comparison of optimal power flow results of the proposed algorithm with other methods found in

Tab. 4: Comparison when optimizing dependent variables.

Methods	Fuel cost ($/h)
EADDE [6]	800.204
DSA [7]	800.388
EEA [5]	800.083
CSA [8]	799.707
EGA [12]	799.5600
BBO [13]	799.1116
KHA [9]	799.0310
MFPA [40]	799.1592
GSA [15]	798.675
GWO	**798.3107**

Tab. 5: Comparison when optimizing dependent variables.

React. Power Gen.	Limits	Qg
Q1	-20 200	-18.7646
G2	-40 50	23.1157
Q5	-40 40	27.3300
Q8	-15 40	33.7790
Q11	-6 24	17.9905
Q13	-6 24	2.55070

Tab. 6: GWO-OPF results comparison for case 1.1.

Pgi (MW)	SA	ISA	KHA	GSO	GWO
P1	173.15	177.124	177.04	174.920	176.9046
P2	48.54	48.933	48.690	44.150	48.7226
P5	19.23	21.3175	21.300	21.760	21.2697
P8	12.81	21.0006	21.080	25.730	21.0509
P11	11.64	11.8605	11.880	11.120	11.8556
P13	12.00	11.860	12.020	13.810	12.0000
Tot. Gn (MW)	277.37	292.095	292.01	291.49	291.8034
Cost ($/h)	799.45	799.277	799.03	799.06	**798.3106**
Losses (MW)	9.200	8.695	8.610	8.48	**8.4034**

the literature as in [3] and [19]. Figure 6(a) shows the voltage profile of case 1.1, without improvement.

2) Case 1.2: OPF with Voltage Profile Improvement

Minimizing only the total fuel cost using OPF problem as in case 1.1; can result in a feasible solution, but voltage profile may not be acceptable. Thus, in this second case, the objective here is to minimize the fuel cost and improving the voltage profile at the same time by minimizing the voltage deviation of PQ buses from the unity 1.0. [36].

The results obtained using the proposed approach are compared with other methods in the literature as shown in Tab. 7 where the total cost found by GWO, in this case, is better than that obtained before.

Figure 4 shows the convergence graph. Figure 5 presents the transmission load flow of the system, from this figure, we can see that the obtained transmission

Tab. 7: Comparison when optimizing dependent variables.

Methods	Fuel cost ($/h)
BBO [13]	804.998
PSO [14]	806.380
DE [1]	805.262
GWO	**806.1530**

loading amounts are within acceptable limits. As we can see from Fig. 6(a), the voltage magnitude is enhanced after the improvement by GWO, and all the load bus voltages are within the permissible range.

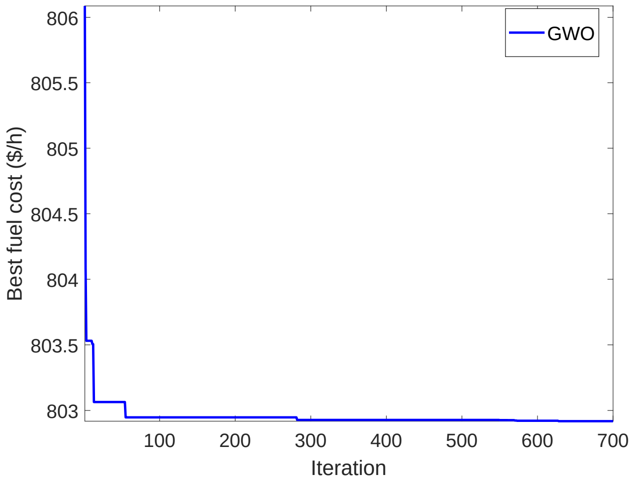

Fig. 4: Convergence characteristic of IEEE30 bus system case 1.2.

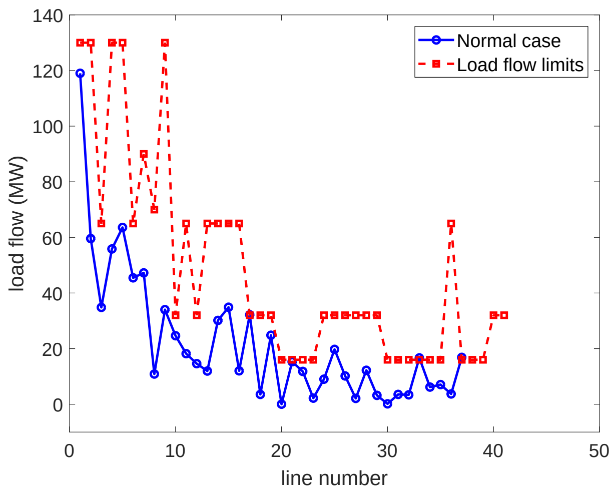

Fig. 5: Transmission Load flows obtained by GWO.

3) Case 1.3: OPF for Fuel Cost Including Valve Point Effect

Considering the same system data as in [23], the valve point effect is incorporated and the fuel cost is evaluated using the Eq. (7). Simulation of power flow results

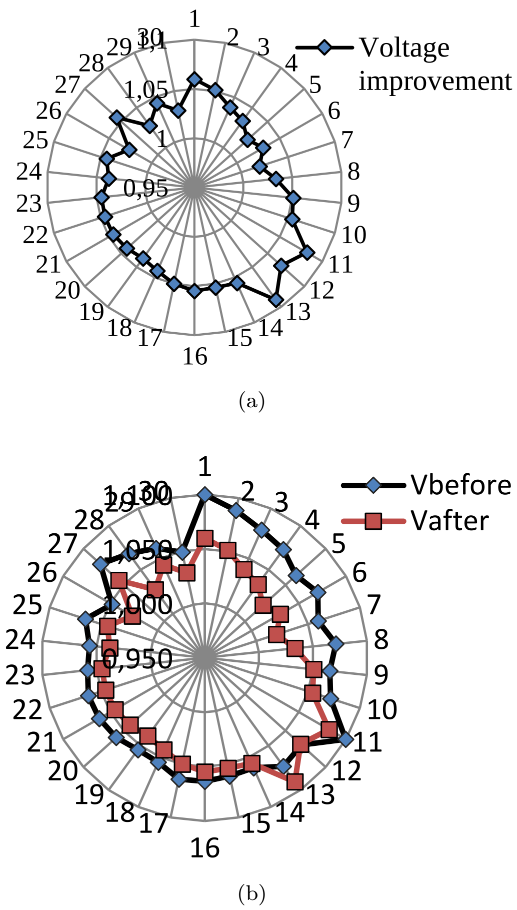

Fig. 6: a) Bus voltage magnitude case 1.2, b) Comparison of voltage profile of IEEE30 bus case 1.1 & case 1.2.

of this case study is compared with other available results as in Tab. 8.

Tab. 8: Obtained results comparison case 1.3.

Methods	Fuel cost (\$/h)
PSO [14]	932.7642
ABC [3]	945.4495
GSA [15]	929.7240
GABC [19]	931.7450
BBO [13]	919.7647
MFPA [40]	917.8298
GWO	**916.6968**

4) Case 1.4: System Analysis Under (N-1) Contingency

To investigate the efficiency of GWO under contingency, a line outage conditions are created on the test system as in [23], in which four contingency conditions are considered (lines: 12–15, 10–20, 15–23 and 6–28). For these four conditions, the voltage profile for normal and contingency conditions is shown in Fig. 7, and corresponding load flow profile is in Fig. 8.

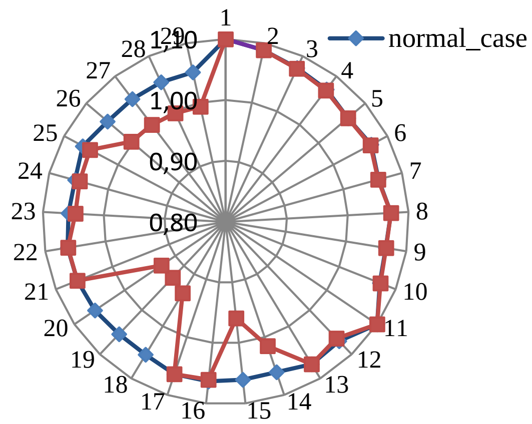

Fig. 7: Voltage profile for normal and contingency conditions.

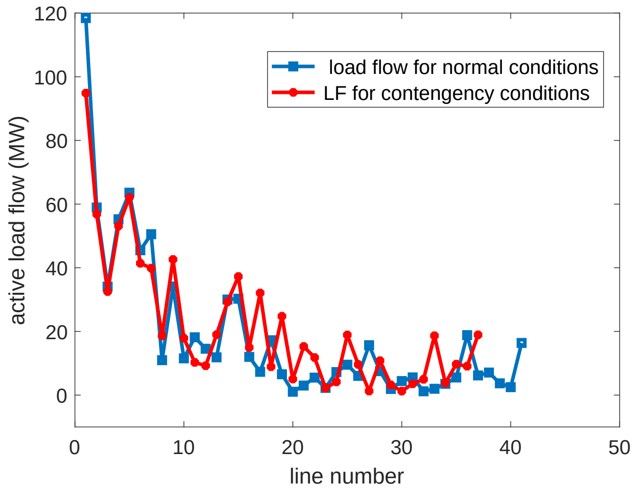

Fig. 8: Load flow profile for normal and contingency conditions.

The load-bus voltages of contingency case are below their normal limit (deviated from their normal limits).To alleviate this problem we apply Eq. (11) and Eq. (12), to bring the voltage at these load buses within 0.95 and 1.05 p.u. Figure 9 shows the corrected voltage profile.

4.2. Case 2: OPF with Wind Energy Case Study

1) Case 2.1: OPF with Stochastic Wind Power Modelling

In this section, GWO algorithm is used to solve OPF problem for system including stochastic wind power in addition to conventional thermal generators. In this case, the system has been modified by replacing conventional generators by wind farms located at buses 5, 11 and 13; each with a total capacity of 60 MW. Two case studies are considered here: in the first case, the wind power is modelled using Weibull distribution

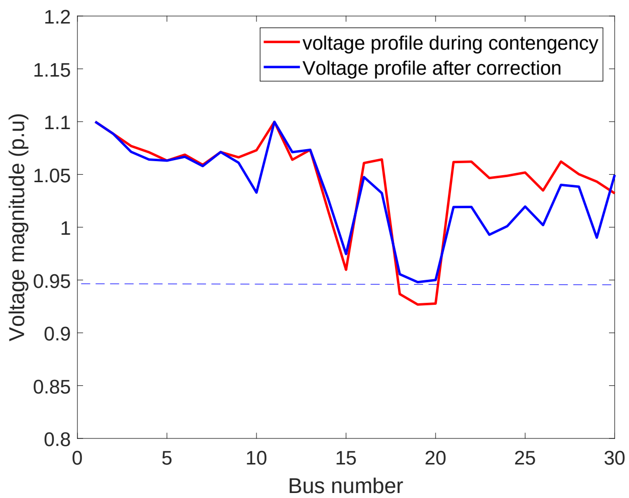

Fig. 9: Voltage profile for normal and contingency conditions.

function in form of imbalance costs of wind power in the main cost objective Eq. (15), which is minimized subject to all given constraints. While, in the second case study, the OPF problem is solved considering different wind speeds.

The test system data given in [23] are taken for this study. The simulation convergence curve and voltage at different buses of the system are given in Fig. 10 and Fig. 11, OPF schedule is given in Tab. 9; the optimal results are then compared with GABC [19] and BFA [23].

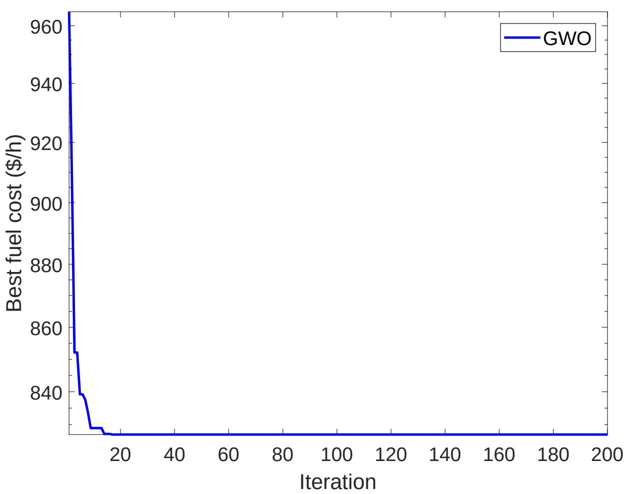

Fig. 10: Convergence graph of fuel cost for wind case.

The obtained results show that the GWO method performs better when compared with other methods for the same case study. The reserved power is higher than the surplus power in Tab. 9, which justifies the fact that the utility service is to purchase an important amount of reserve for covering any unavailable wind energy.

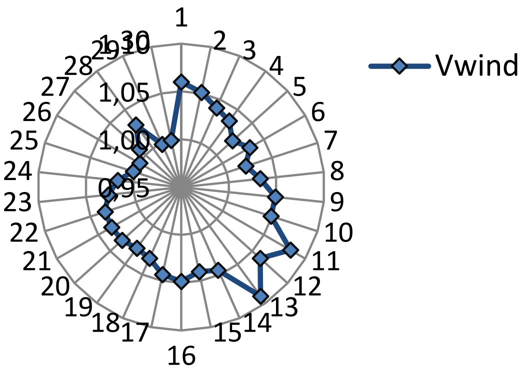

Fig. 11: Bus voltage magnitude for wind case.

Tab. 9: Simulation results for wind case study.

Pgi (MW)	GABC [19]	BFA [23]	GWO	Reserved real power	Excess power
P1	50.219	56.530	50.524		
P2	20.581	34.285	20.461		
PWIND1	60.000	50.729	59.995	40.411	0.001
P8	35.000	65.956	34.976		
PWIND2	60.000	40.405	60.000	26.783	0
PWIND3	59.999	39.162	59.904	25.550	0.029
Total. Gen. (MW)	285.80	287.06	285.86		
Cost ($/h)	819.293	947.50	**826.82**		
Losses (MW)	-	-	**2.4144**		

As seen from Fig. 10, the total fuel cost is decreased by the integration of wind power source in the system.

2) Case 2.2: OPF Study with Wind Energy Considering Reserve Constraints

Case 2.2.1: OPF without Wind Power

In this case study, we used the same configuration as in [2], by considering the nodes 1, 2, 13, 22, 23 and 27 as generator buses and total system load of 189.2 MW. First, we proceeded for optimal power flow without wind energy; the simulation results of this case are compared to those reported in [2], as shown in Tab. 10.

It can be noticed that the obtained GWO cost is better comparing with the case without wind power.

Case 2.2.2: Wind Energy with Zero Cost

Two scenarios of wind power integration levels are considered in this study; 10 %, and 20 % of the system load. These levels are connected to bus 8. Using Eq. (25), Eq. (26) and Eq. (27), we calculated the spinning reserve under different wind speeds at the second hour, assuming the wind speed at the first hour was 3 $m \cdot s^{-1}$.

Tab. 10: Simulation results for wind case with spinning reserve.

Wind speed	UP/Down Spinning reserve requirements for wind power Conditions (MW)			UP/Down Spinning reserve capacity supplied by thermal units (MW)		Total cost ($/h)
Scenario 1	**USR**	**DSR**	**Pw (MW)**	**USR**	**DSR**	
4	28.964	0.584	1.169	55.000	47.008	569.8760
5	29.829	1.449	2.899	55.000	46.575	563.1616
6	30.993	2.613	5.227	55.000	45.993	554.1656
7	32.292	3.912	7.824	55.000	45.344	544.1806
8	33.635	5.255	10.511	55.000	44.672	533.9034
Scenario 2	**USR**	**DSR**	**Pw (MW)**	**USR**	**DSR**	
4	29.614	1.234	2.469	55.000	46.683	564.8280
5	31.325	2.945	5.897	55.000	45.827	551.5847
6	33.678	5.225	10.45	55.000	44.687	534.1380
7	36.265	7.885	15.77	55.000	43.357	513.9586
8	38.899	10.51	21.02	55.000	42.045	494.2616

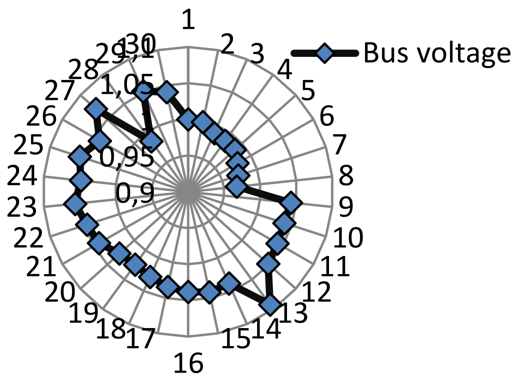

Fig. 12: Voltage profile at different nodes for modified system.

Tab. 11: OPF results of modified IEEE30 bus system.

Pgi (MW)	GWO Without wind	EPSO [2]
P1	43.4397	43.425
P2	57.7903	55.785
P13	17.4824	17.716
P22	23.0944	23.131
P22	17.2086	18.241
P27	32.6450	33.307
W1	-	-
Total gen. (MW)	**191.6604**	191.605
Cost ($/h)	**574.7271**	574.766
Losses (MW)	**2.4604**	2.408
Voltage div	1.0572	

The spinning reserve of the system was $s = 15$ % of the total demand, and the up-spinning reserve was set to improve the safety of the power system operation under wind intermittent conditions or uncertain wind power. Simulation results for wind case study.

This was achieved by using Eq. (27), in which this reserve constraint of wind generation was $r = 50$ % of the system load. After computing the wind power using Eq. (25), we run the OPF program to calculate the cost associated with this wind injection then we proceeded to the calculation of different spinning reserve constraint limits, the obtained results are depicted in Tab. 10.

The wind speeds values were respectively 4, 5, 6, 7, and 8 $\text{m}\cdot\text{s}^{-1}$; different computation results of scenarios 1 and 2 are presented in Tab. 12 and the system voltage profile is shown in Fig. 13.

Tab. 12: Simulation results for wind case study.

Wind speed ($\text{m}\cdot\text{s}^{-1}$)	**4**	**5**	**6**	**7**	**8**
Scenario 1(10 % of wind penetration)					
Cost ($/h)	571.24	571.565	581.487	605.395	644.38
Scenario 2 (20 % of wind penetration)					
Cost ($/h)	570.92	586.359	643.340	762.651	936.10

Case 2.2.3: OPF Considering Wind Power Cost

In this case, we assume that the wind power has the same direct cost of [19] $d_1 = 1$ $/h, without considering the imbalance cost. Simulation results for wind case study.

The simulation result is shown in Tab. 12, we can see that when wind speed increases, the total operation cost increases too, due to the wind direct cost impact on the total operating cost.

4.3. Case 3: OPF with Stochastic Wind Speed

In this case study and in order to check the effect of uncertain wind power on the test power system, two wind farms each with capacity of 30 MW have been connected at two separate locations; at nodes 26 and node 30 as in [19]. The results obtained are then compared with the case without wind energy.

Two cases are considered here; the first one where the scale factor "c" takes the values of 3 to 30 while keeping the shape factor at $k = 2$, then by keeping the scale factor constant at the value 10 and varying the reserve coefficient (Krw) from its base value of 4, and with the installed wind power capacity for each wind farm of 20 MW instead of 30 MW by applying the proposed approach taking into consideration these conditions, we find the results as shown in Fig. 13(a).

For the second case study, we maintained the values of wind turbines Weibull model factors constant, $v_in = 4$ m·s^{-1}, $v_r = 12$ m·s^{-1}, $v_{out} = 25$ m·s^{-1}, $c = 3$, $k = 2$, $K_{pw} = 1$, $K_{rw} = 4$, but considering the direct costs of the two wind farms $d1 = d2 = 1.3$ \$/h. Simulation results are presented in Tab. 13, the convergence characteristics for different values of reserve coefficient "K_{rw}" is given in Fig. 13(b).

Generally, the direct cost of wind power is less than the average cost of thermal power, and the penalty cost of not using all the available wind power is considered less than the direct cost. From Fig. 13(b), it can be seen that, the larger the value of c the higher the value of wind speed and hence wind power penetration amount. However, the amount of wind power injected at bus 26 remains, less than that injected at bus 30, due to the thermal loading limit of the transmission line at this section.

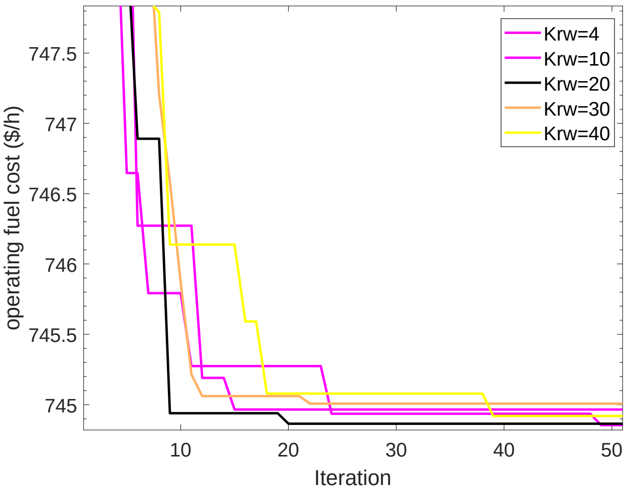

(a)

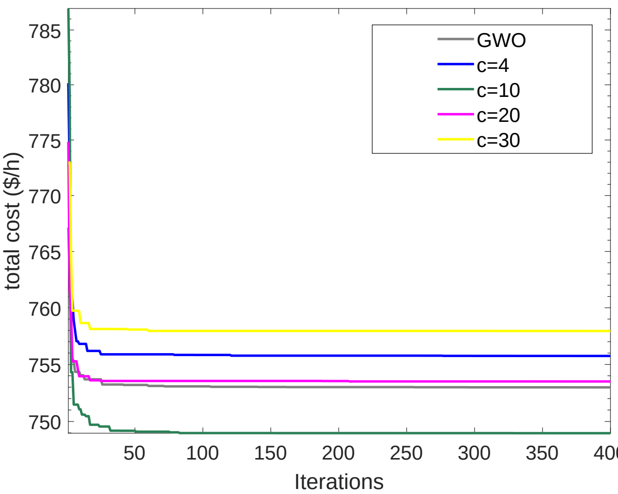

(b)

Fig. 13: Convergence characteristic for a) different values of reserve coefficient (K_{rw}), b) different values of scale factor "c".

Tab. 13: Simulation results for wind case study.

Pgi (MW)	**With -out wind**	**With wind (c=2, k=2)**	**With wind (c=10, k=10, $K_{rw}=4$)**	**With wind (c=10, k=2, $K_{rw}=30$)**
P1	176.1721	143.002	156.945	156.87
P2	48.0926	40.799	44.029	44.053
P5	21.1376	18.943	19.957	19.984
P8	23.3591	10.000	10.000	10.018
P11	11.3591	10.019	10.000	10.013
P13	12.0000	12.026	12.000	12.014
W1	-	29.942	20.000	19.958
W2	-	30.000	20.989	20.000
Total. Gen. (MW)	292.1205	294.731	292.931	292.61
Cost (\$/h)	**801.176**	**741.514**	**744.821**	**744.82**
Losses (MW)	**9.180**	**11.327**	**9.5230**	**9.5123**
Voltage div.		0.108	0.108	0.1084
Wind Over_E MW		**26.69**	**25.321**	**25.302**

4.4. Case Study N°2: IEEE57 Bus Test System

This system consists of 7 thermal generators, with bus 1 is considered as slack bus; 2, 3, 6, 8, 9 and 12 as PV buses, 50 load buses and 80 lines, among which 17 lines are equipped with tap changing transformers. In addition, three shunt Var compensators are installed at buses 18, 25 and 53. The system data are taken from [37]. Two cases are investigated in this case study:

1) Case 1: OPF for Quadratic Fuel Cost

In this case study, the objective function to be optimized is represented by the quadratic fuel cost, related to thermal generators unit described by the Eq. (6).

The optimal power flow for the first case study using GWO takes the settings of the algorithm as the followings: search agent number equals to 30, and the number of runs equals to 300. These are the same system settings used for the other methods, and the obtained simulation results are shown in Tab. 14.

Tab. 14: Optimal control variables settings for case 1.

Control variables	Lower/ upper limits	Case 1	Control variables	Case 1
P1(MW)	0 576	143.7886	T24-25	1.0125
P2	0 150	89.7403	T25-26	1.0000
P3	0 120	45.1711	T7-29	1.0125
P6	0 100	72.1034	T34-32	0.9125
P8	0 300	459.8802	T11-41	0.9000
P9	0 120	94.9161	T15-45	1.0125
P12	0 300	360.4463	T14-46	0.9875
V1	0.95–1.05	1.0499	T10-51	1.0000
V2	0.95–1.10	1.0479	T13-49	0.9625
V3	0.95–1.10	1.0408	T11-43	0.9625
V6	0.95–1.10	1.0493	T40-56	0.9625
V8	0.95–1.10	1.0342	T39-57	0.9625
V9	0.95–1.10	1.0332	T9-55	0.9875
V12	0.95–1.10	1.0406	Qsc1	1.0170
T4-18	0.90–1.10	0.9375	Qsc1	0.9070
T4-18	0.90–1.10	1.0500	Qsc2	0.9680
T21-20	0.90–1.10	0.9750	-	-
Fuel cost ($/h)	-	**41683.5076**		-
Power loss (MW)	-	**15.2460**		-

The results obtained by the proposed method were compared with others available methods, this comparison shows that the GWO algorithm gives better results when compared to many algorithms found in the literature as shown in Tab. 15.

Tab. 15: Comparison of fuel costs case 1.

Methods	Fuel cost ($/h)
TSA [41]	41685.07
HS [38]	41693.358
ABC [3]	41693.958
BBO [13]	41721.246
MATPOWER [37]	41737.790
EADDE [6]	41713.620
GSA [15]	41695.8717
KHA [9]	41709.2647
GWO	**41683.5076**

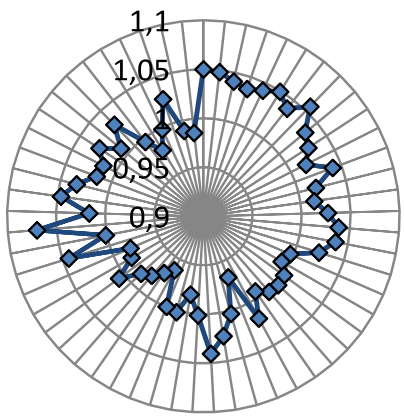

Fig. 14: Bus voltage profile for IEEE57 case 1.

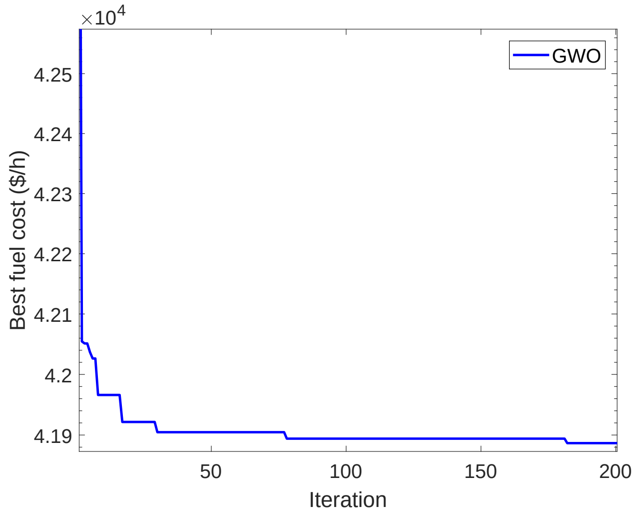

Fig. 15: Convergence curve for IEEE57 case 1.

2) Case 2: OPF with Voltage Profile Improvement of IEEE57 Test System

Bus voltage enhancement is one of the most significant safety and service qualification indices. In order to assess this case, a two-fold objective function is considered to minimize the operating fuel cost and enhancing the voltage profile at the same time by minimizing all the load bus deviations from the reference value. Voltage profile, in this case, is compared to that of the precedent one as shown in Fig. 16 and the operating cost curve is shown in Fig. 17.

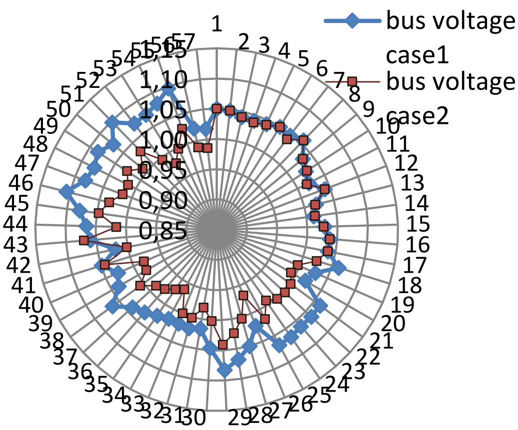

Fig. 16: Voltage improvement profile comparison.

It is clear that the voltage profile is enhanced efficiently compared with that in case 1. This could be achieved by the optimal tuning of the control parameters within the constraints range as given in Tab. 16 using the proposed GWO technique.

It can be seen that the proposed GWO method converges to a better result than EADDE [7] method by decreasing the fuel cost from 42051.44 $/h to

Tab. 16: Performances measures for the TFC ($/h) in both cases.

System	IEEE 30-bus system				IEEE 57-bus system			
Method	**GWO**	**EADDE [6]**	**MDE [35]**	**PSO [14]**	**GWO**	**TSA [41]**	**ABC [3]**	**PSO [14]**
Min	798.2934	800.204	802.376	800.409	41,684.00	41,685.07	41,781.00	41,688.68
Mean	798.6380	800.241	802.382	800.450	41,686.00	41,687.78	41,840.00	41,697.58
Max	800.1367	800.278	802.404	801.231	41,688.29	41,689.05	41,927.00	41,727.86
runs	40	30	40	20	50	50	20	20

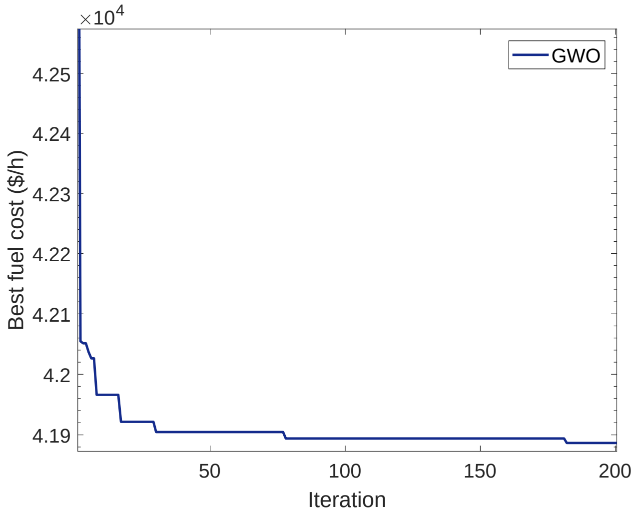

Fig. 17: Convergence curve for IEEE57 in case 2.

41817.3826 $/h and voltage deviation from 0.7882 to 0.74.

Tab. 17: Optimal control variables settings for case 2.

Control variables	Case 2	Control variables	Case 2
P1	142.189	T24-25	0.9033
P2	89.894	T24-25	0.9767
P3	45.148	T24-26	1.0279
P6	72.928	T7-29	0.9861
P8	459.393	T34-32	0.9210
P9	84.089	T11-41	0.9368
P12	363.088	T15-45	0.9713
V1	1.0212	T14-46	0.9720
V2	1.0740	T10-51	0.9933
V3	1.0646	T13-49	0.9327
V6	0.9913	T11-43	0.9397
V8	1.0519	T40-56	1.0269
V9	1.0808	T39-57	0.9504
V12	1.0103	T9-55	0.9976
T4-18	1.0760	Qsc1	1.1419
T4-18	0.9313	Qsc1	0.2719
T21-20	1.0032	Qsc2	0.4971
Fuel cost ($/h)	**41817.382**		
Power loss (MW)	**16.1146**		-
Voltage div. (p.u)	**0.74**		

From the comparison of the results shown in Tab. 16, it can be concluded that the solution quality of the GWO algorithm is very competitive and challenging because it converges to the best solution with less computational time. Figure 18 presents the convergence curve for IEEE30 bus system after 40 runs and Fig. 19 the convergence curve for IEEE57-bus system after 50 runs.

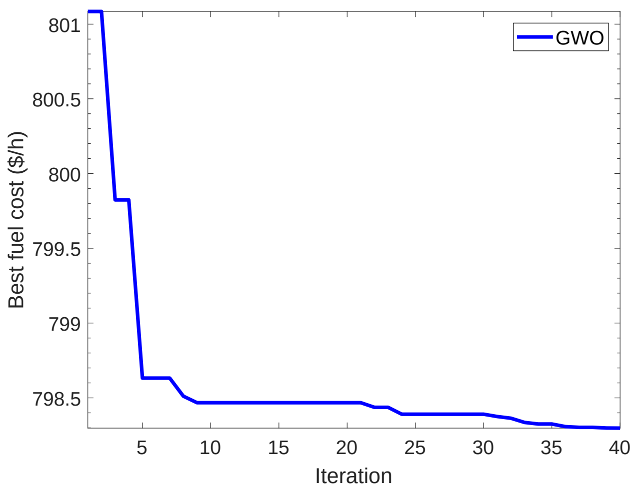

Fig. 18: Convergence curves for IEEE57 with 50 runs.

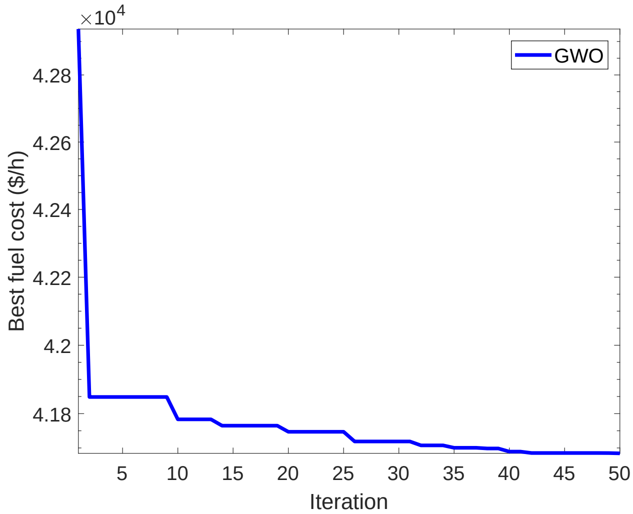

Fig. 19: Convergence curves for IEEE57 with 50 runs.

5. Conclusion

This paper presents an optimal power flow study using a new meta-heuristic population-based search algorithm called Grey Wolf Optimizer (GWO). Considering both wind and thermal power generators, in order to evaluate the effectiveness of the proposed technique; three case studies are considered in this work.

By adding to the normal operation condition, the N-1 contingency condition represented by lines outage and the uncertainty of wind power, which is modelled using Weibull distribution function is investigated.

Simulations results obtained by OPF analysis for two standard test systems IEEE-30, and IEEE-57 bus systems without considering wind power are compared with results of other methods available in the literature. The outcome of the comparison confirms the effectiveness and robustness of the proposed algorithm.

Similarly, the results obtained in presence of wind energy system were compared with those of other methods reported in the literature using the IEEE 30 bus system. By increasing the value of reserve coefficient, the value of the injected amount in the system can be limited by the transmission system permissible capacity of the existing network. On the other hand; when increasing the wind penetration level by increasing wind speed, the total operating cost decreases.

The method presents compromising performances measures compared to other methods found in the literature. This analysis will be extended in the future to include spinning reserve in the main optimal power flow problem.

References

[1] ABOU, A. A., M. A. ABIDO and S. R. SPEA. Optimal power flow using differential evolution algorithm. *Electrical Engineering*. 2009, vol. 91, iss. 2, pp. 69–78. ISSN 0948-7921. DOI: 10.1007/s00202-009-0116-z.

[2] CHANG, Y. C., T. Y. LEE, C. L. CHEN and R. M. JAN. Optimal power flow of a wind-thermal generation system. *International Journal of Electrical Power & Energy Systems*. 2014, vol. 55, iss. 1, pp. 312–320. ISSN 0142-0615. DOI: 10.1016/j.ijepes.2013.09.028.

[3] REZAEI, M. and A. KARAMI. Artificial bee colony algorithm for solving multi-objective optimal power flow problem. *International Journal of Electrical Power & Energy Systems*. 2013, vol. 53, iss. 1, pp. 219–230. ISSN 0142-0615. DOI: 10.1016/j.ijepes.2013.04.021.

[4] BAKIRTZIS, A. G., P. N. BISKAS, C. E. ZOUMAS and V. PETRIDIS. Optimal power flow by enhanced genetic algorithm. *IEEE Transactions on Power Systems*. 2002, vol. 17, iss. 2, pp. 229–236. ISSN 0885-8950. DOI: 10.1109/tpwrs.2002.1007886.

[5] SURENDER, S. R., P. R. BIJWE and A. R. ABHYANKAR. Faster evolutionary algorithm base optimal power flow using incremental variables. *Electrical Power and Energy System*. 2014, vol. 54, iss. 1, pp. 198–210. ISSN 0142-0615. DOI: 10.1016/j.ijepes.2013.07.019.

[6] VAISAKH, K. and L. R. SRINIVAS. Evolving ant direction differential evolution for OPF with non-smooth cost functions. *Engineering Applications of Artificial Intelligence*. 2011, vol. 24, iss. 3, pp. 426–436. ISSN 0952-1976. DOI: 10.1016/j.engappai.2010.10.019.

[7] ABACI, K. and V. YAMACLI. Differential search algorithm for solving multi-objective optimal power flow problem. *International Journal of Electrical Power & Energy Systems*. 2016, vol. 79, iss. 1, pp. 1–10. ISSN 0142-0615. DOI: 10.1016/j.ijepes.2015.12.021.

[8] GHASEMI, M., S. GHAVIDEL, M. GITIZADEH and E. AKBARI. An improved teaching–learning-based optimization algorithm using Levy mutation strategy for non-smooth optimal power flow. *International Journal of Electrical Power & Energy Systems*. 2015, vol. 65, iss. 1, pp. 375–384. ISSN 0142-0615. DOI: 10.1016/j.ijepes.2014.10.027.

[9] ROY, P. K. and C. PAUL. Optimal power flow using krill herd algorithm. *International Transactions on Electrical Energy Systems*. 2015, vol. 25, iss. 8, pp. 1397–1419. ISSN 2050-7038. DOI: 10.1002/etep.1888.

[10] ROA-SEPULVEDA, C. A. and B. J. PAVEZ-LAZO. A solution to the optimal power flow using simulated annealing. In: *IEEE Porto Power Tech Proceedings*. Porto: IEEE, 2001, pp. 5–9. ISBN 0-7803-7139-9. DOI: 10.1109/PTC.2001.964733.

[11] BENTOUATI, B., S. CHETTIH, L. CHAIB and V. SREERAM. Interior search algorithm for optimal power flow with non-smooth cost functions. *Cogent Engineering*. 2017, vol. 4, iss. 1, pp. 1–17. ISSN 2331-1916. DOI: 10.1080/23311916.2017.1292598.

[12] KUMARI, M. S. and S. MAHESWARAPU. Enhanced Genetic Algorithm based computation technique for multi-objective Optimal Power Flow solution. *International Journal of Electrical Power & Energy Systems*. 2010, vol. 32, iss. 6, pp. 736–742. ISSN 0142-0615. DOI: 10.1016/j.ijepes.2010.01.010.

[13] BHATTACHARYA, A. and P. K. CHATTOPADHYAY. Application of biogeography-based optimisation to solve different optimal power flow problems. *IET Generation, Transmission & Distribution*. 2011, vol. 5, iss. 1, pp. 70–80. ISSN 1751-8687. DOI: 10.1049/iet-gtd.2010.0237.

[14] ABIDO, M. A. Optimal power flow using particle swarm optimization. *International Journal of Electrical Power & Energy Systems*. 2002, vol. 24, iss. 7, pp. 563–571. ISSN 0142-0615. DOI: 10.1016/S0142-0615(01)00067-9.

[15] DUMAN, S., U. GUVENC, Y. SONMEZ and N. YORUKEREN. Optimal power flow using gravitational search algorithm. *Energy Conversion and Management*. 2012, vol. 59, iss. 1, pp. 86–95. ISSN 0196-8904. DOI: 10.1016/j.enconman.2012.02.024.

[16] VAISAKH, K., L. R. SRINIVAS and K. MEAH. Genetic evolving ant direction PSODV hybrid algorithm for OPF with non-smooth cost functions. *Electrical Engineering*. 2013, vol. 95, iss. 3, pp. 185–199. ISSN 0948-7921. DOI: 10.1007/s00202-012-0251-9.

[17] KUMAR, R. A. and L. PREMALATHA. Optimal power flow for a deregulated power system using adaptive real coded biogeography-based optimization. *International Journal of Electrical Power & Energy Systems*. 2015, vol. 73, iss. 1, pp. 393–399. ISSN 0142-0615. DOI: 10.1016/j.ijepes.2015.05.011.

[18] KHAMEES, K. A., A. E. RAFEI, N. M. BADRA and A. Y. ABDELAZIZ. Solution of optimal power flow using evolutionary-based algorithms. *International Journal of Engineering, Science and Technology*. 2017, vol. 9, no. 1, pp. 55–68. ISSN 2141-2839.

[19] ROY, R. and H. T. JADHAV. Optimal power flow solution of power system incorporating stochastic wind power using Gbest guided artificial bee colony algorithm. *International Journal of Electrical Power & Energy Systems*. 2015, vol. 64, no. 1, pp. 562–578. ISSN 0142-0615. DOI: 10.1016/j.ijepes.2014.07.010.

[20] MASKAR, M. B., A. R. THORAT, P. D. BAMANE and I. KORACHGAON. Optimal power flow incorporating thermal and wind power plant. In: *International Conference on Circuit, Power and Computing Technologies*. Kollam: IEEE, 2017, pp. 1–6. ISBN 978-1-5090-4967-7. DOI: 10.1109/ICCPCT.2017.8074265.

[21] JIANG, S., Z. JI and Y. WANG. A novel gravitational acceleration enhanced particle swarm optimization algorithm for wind–thermal economic emission dispatch problem considering wind power availability. *International Journal of Electrical Power & Energy Systems*. 2015, vol. 73, iss. 1, pp. 1035–1050. ISSN 0142-0615. DOI: 10.1016/j.ijepes.2015.06.014.

[22] PANDA, A. and M. TRIPATHY. Security constrained optimal power flow solution of wind-thermal generation system using modified bacteria foraging algorithm. *Energy*. 2015, vol. 93, iss. 1, pp. 816–827. ISSN 0360-5442. DOI: 10.1016/j.energy.2015.09.083.

[23] MISHRA, S., Y. MISHRA and S. VIGNESH. Security constrained economic dispatch considering wind energy conversion systems. In: *IEEE Power and Energy Society General Meeting*. Detroit: IEEE, 2011, pp. 1–8. ISBN 978-1-4577-1000-1. DOI: 10.1109/PES.2011.6039544.

[24] SULAIMAN, M. H., Z. MUSTAFFA, M. R. MOHAMED and O. ALIMAN. Using the gray wolf optimizer for solving optimal reactive power dispatch problem. *Applied Soft Computing*. 2015, vol. 32, iss. 1, pp. 286–292. ISSN 1568-4946. DOI: 10.1016/j.asoc.2015.03.041.

[25] EL-FERGANY, A. A. and H. M. HASANIEN. Single and Multi-objective Optimal Power Flow Using Grey Wolf Optimizer and Differential Evolution Algorithms. *Electric Power Components and Systems*. 2015, vol. 43, iss. 13, pp. 1548–1559. ISSN 1532-5008. DOI: 10.1080/15325008.2015.1041625.

[26] IAHKALI, H. and M. VAKILIAN. Stochastic unit commitment of wind farms integrated in power system. *Electric Power Systems Research*. 2010, vol. 80, iss. 9, pp. 1006–1017. ISSN 0378-7796. DOI: 10.1016/j.epsr.2010.01.003.

[27] MIRJALILI, S., S. M. MIRJALILI and A. LEWIS. Grey Wolf Optimizer. *Advances in Engineering Software*. 2014, vol. 69, iss. 9, pp. 46–61. ISSN 0965-9978. DOI: 10.1016/j.advengsoft.2013.12.007.

[28] MIRJALILI, S. and S. Z. M. HASHIM. A new hybrid PSOGSA algorithm for function optimization. In: *International Conference on Computer and Information Application*. Tianjin: IEEE, 2010, pp. 374–377. ISBN 978-1-4244-8598-7. DOI: 10.1109/ICCIA.2010.6141614.

[29] BAI, W., D. LEE and K. LEE. Stochastic Dynamic Optimal Power Flow Integrated with Wind Energy Using Generalized Dynamic Factor Model. *IFAC-Papers OnLine*. 2016, vol. 49, iss. 27, pp. 129–134. ISSN 2405-8963. DOI: 10.1016/j.ifacol.2016.10.731.

[30] XIE, L., H. D. CHIANG and S. H. LI. Optimal power flow calculation of power system with wind farms. In: *IEEE Power and Energy Society General Meeting*. Detroit: IEEE, 2011, pp. 1–6. ISBN 978-1-4577-1000-1. DOI: 10.1109/PES.2011.6039105.

[31] MONDAL, S., A. BHATTACHARYA and S. H. NEE-DEY. Multi-objective economic emission load dispatch solution using gravitational search algorithm and considering wind power penetration. *International Journal of Electrical Power & Energy Systems*. 2013, vol. 44, iss. 1, pp. 282–292. ISSN 0142-0615. DOI: 10.1016/j.ijepes.2012.06.049.

[32] MOHAMED, A. A., A. M. EL-GAAFARY, Y. S. MOHAMED and A. M. HEMEIDA. Multi-objective Modified Grey Wolf Optimizer for Optimal Power Flow. In: *Eighteenth International Middle East Power Systems Conference (MEPCON)*. Cairo: IEEE, 2016, pp. 982–990. ISBN 978-1-4673-9063-7. DOI: 10.1109/MEPCON.2016.7837016.

[33] KAPOOR, S., I. ZEYA, C. SINGHAL and S. J. NANDA. A Grey Wolf Optimizer Based Automatic Clustering Algorithm for Satellite Image Segmentation. *Procedia Computer Science*. 2017, vol. 115, iss. 1, pp. 415–422. ISSN 1877-0509. DOI: 10.1016/j.procs.2017.09.100.

[34] ANANTASATE, S. and P. BHASAPUTRA. A multi-objective bees algorithm for multi-objective optimal power flow problem. In: *The 8th Electrical Engineering/ Electronics, Computer, Telecommunications and Information Technology (ECTI) Association of Thailand*. Khon Kaen: IEEE, 2011, pp. 852–856. ISBN 978-1-4577-0425-3. DOI: 10.1109/ECTICON.2011.5947974.

[35] SAYAH, S. and K. ZEHAR. Modified differential evolution algorithm for optimal power flow with non-smooth cost functions. *Energy Conversion and Management*. 2008, vol. 49, iss. 11, pp. 3036–3042. ISSN 0196-8904. DOI: 10.1016/j.enconman.2008.06.014.

[36] BOUCHEKARA, H. R. E. H. Optimal power flow using black-hole-based optimization approach. *Applied Soft Computing*. 2014, vol. 24, iss. 1, pp. 879–888. ISSN 1568-4946. DOI: 10.1016/j.asoc.2014.08.056.

[37] ZIMMERMAN, R., C. MURILLO-SANCHEZ and D. GAN. *Matlab power System Simulation Package*. New York: School of Electrical Engineering, Cornell University, 2007.

[38] SINSUPAN, N., U. LEETON and T. KULWORAWANICHPONG. Application of harmony search to optimal power flow problems. In: *International Conference on Advances in Energy Engineering*. Beijing: IEEE, 2010, pp. 219–222. ISBN 978-1-4244-7831-6. DOI: 10.1109/ICAEE.2010.5557575.

[39] REDDY, S. S., and C. SRINIVASA RATHNAM. Optimal Power Flow using Glowworm Swarm Optimization. *International Journal of Electrical Power & Energy Systems*. 2016, vol. 80, iss. 1, pp. 128–139. ISSN 0142-0615. DOI: 10.1016/j.ijepes.2016.01.036.

[40] REGALADO, J. A., B. E. EMILIO and E. CUEVAS. Optimal power flow solution using Modified Flower Pollination Algorithm. In: *IEEE International Autumn Meeting on Power, Electronics and Computing*. Ixtapa: IEEE, 2015, pp. 1–6. ISBN 978-1-4673-7121-6. DOI: 10.1109/ROPEC.2015.7395073.

[41] EL-FERGANY, A. A. and H. M. HASANIEN. Tree-seed algorithm for solving optimal power flow problem in large-scale power systems incorporating validations and comparisons. *Applied Soft Computing*. 2018, vol. 64, iss. 1, pp. 307–316. ISSN 1568-4946. DOI: 10.1016/j.asoc.2017.12.026.

About Authors

Sebaa HADDI was born in Setif, Algeria. He received his M.Sc. from University of Setif in 1997. follows his study in the University of Ferhat Abbes Setif 1, has got his B.Sc. degree in Electrical Engineering Power system from Setif University (Algeria) in 1997, and his M.Sc. degree in 2009 in the field of electrical network, now he prepares for the Doctorate degree in the Department of Electrical Engineering, of the university of Setif, His research interests include the optimization in power system, optimal integration of renewable sources, Facts device.

Omrane BOUKETIR was born in Setif, Algeria. He received his M Eng. in Electrical Automation from Setif University (Algeria) in 1995. In 1999 he obtained his M.Sc. degree from University Putra Malaysia in the field of Automation and Robotics and Ph.D. degree in power electronics systems from the same university in 2005. His research areas include power electronics and drive systems, SiC switching devices, CAD tools in electrical engineering and trends and methods in tertiary education.

Tarek BOUTKIR was born in Setif, Algeria. He received his M.Sc. in Electrical Engineering Power system from Setif University (Algeria) in 1994, his

M.Sc. degree from Annaba University in 1998, his Ph.D. degree in power system from Batna University (Algeria) in 2003. His areas of interest are the application of the meta-heuristic methods in optimal power flow, FACTS control and improvement in electric power systems, Multi-Objective Optimization for power systems, and Voltage Stability and Security Analysis. He is the Editor-In-Chief of Journal of Electrical Systems (Algeria), the Co-Editor of Journal of Automation & Systems Engineering (Algeria).